Deterministic and Ensemble-Based Spatially-Coupled Product Codes

Christian Häger[†], Henry D. Pfister[‡], Alexandre Graell i Amat[†], and Fredrik Brännström[†]
[†]Department of Signals and Systems, Chalmers University of Technology, Gothenburg, Sweden
[‡]Department of Electrical and Computer Engineering, Duke University, Durham, North Carolina

Abstract—Several authors have proposed spatially-coupled (or convolutional-like) variants of product codes (PCs). In this paper, we focus on a parametrized family of generalized PCs that recovers some of these codes (e.g., staircase and block-wise braided codes) as special cases and study the iterative decoding performance over the binary erasure channel. Even though our code construction is deterministic (and not based on a randomized ensemble), we show that it is still possible to rigorously derive the density evolution (DE) equations that govern the asymptotic performance. The obtained DE equations are then compared to those for a related spatially-coupled PC ensemble. In particular, we show that there exists a family of (deterministic) braided codes that follows the same DE equation as the ensemble, for any spatial length and coupling width.

I. INTRODUCTION

Several authors have proposed modifications of the classical product code (PC) construction by Elias [1], typically by considering nonrectangular code arrays. These modifications can be regarded as generalized low-density parity-check (LDPC) codes [2], where the underlying Tanner graph consists exclusively of degree-2 variable nodes (VNs). We refer to such codes as generalized PCs (GPCs). For example, GPCs have been investigated by many authors as practical solutions for high-speed fiber-optical communications [3]–[7].

For the binary erasure channel (BEC), we are interested in the asymptotic iterative decoding performance of GPCs whose associated code arrays have a spatially-coupled or convolutional-like structure. Examples include braided codes [5], [8] and staircase codes [4]. Spatially-coupled codes have attracted significant attention in the literature due to their outstanding performance under iterative decoding [9], [10].

An asymptotic analysis is typically based on density evolution (DE) [11], [12] using an ensemble argument. This approach was taken for spatially-coupled PCs in [13], [14]. However, a randomly chosen code from these ensembles is unlikely to have a product array (row-column) structure and hence does not resemble the codes that are implemented in practice, e.g., staircase or braided codes. It is thus desirable to make precise statements about the performance of sequences of deterministic (and structured) GPCs.

We consider the high-rate regime, where one assumes that component codes correct a fixed number of erasures and then

studies the case where the component code length n tends to infinity. Using a Chernoff bound, one finds that for any fixed erasure probability p, the decoding will fail for large n with high probability. Therefore, it is customary to let the erasure probability decay slowly as c/n for some $c > 0$. This leads to rigorous decoding thresholds in terms of c which may be interpreted as the effective channel quality. The high-rate regime is also the regime that is relevant in practice: It is at high rates where GPCs are competitive compared to LDPC codes and practical GPCs typically employ long component codes with small erasure-correcting capability [3]–[5].

The main contribution of this paper is to show that, analogous to DE for code ensembles, there exists a large class of deterministic GPCs whose asymptotic performance in the high-rate regime is rigorously characterized in terms of a recursive DE equation. The code construction we propose here is sufficiently general to recover (block-wise) braided and staircase codes as special cases. Our result generalizes previous work in [3] from conventional PCs to a large class of deterministic GPCs. We further provide a detailed comparison between deterministic spatially-coupled PCs and the ensembles in [13], [14] via their respective DE equations. For example, we show that there exists a family of block-wise braided codes that follows the same DE recursion as the ensemble in [13]. This implies that certain ensemble-properties proved in [13] also apply to deterministic GPCs.

Notation. We use boldface letters to denote vectors and matrices (e.g., $\boldsymbol{x}$ and $\boldsymbol{A}$). The symbols $\boldsymbol{0}_m$ and $\boldsymbol{1}_m$ denote the all-zero and all-one vectors of length m, where the subscript may be omitted. The tail-probability of a Poisson random variable is defined as $\Psi_{\geq t}(x) \triangleq 1 - \sum_{i=0}^{t-1} \Psi_{=i}(x)$, where $\Psi_{=i}(x) \triangleq \frac{x^i}{i!} e^{-x}$. We use boldface to denote the element-wise application of a scalar-valued function to a vector, e.g., $\boldsymbol{\Psi}_{\geq t}(\boldsymbol{x})$ applies $\Psi_{\geq t}(\cdot)$ to each element in $\boldsymbol{x}$. For vectors, we use $\boldsymbol{x} \succeq \boldsymbol{y}$ if $x_i \geq y_i$ for all i. We define $[m] \triangleq \{1, 2, \ldots, m\}$. The indicator function is denoted by $\mathbb{1}\{\cdot\}$.

II. CODE CONSTRUCTION AND DENSITY EVOLUTION FOR DETERMINISTIC GENERALIZED PRODUCT CODES

We denote a GPC by $\mathcal{C}_n(\boldsymbol{\eta})$, where n is proportional to the number of constraint nodes (CNs) in the underlying Tanner graph and $\boldsymbol{\eta}$ is a binary, symmetric $L \times L$ matrix that defines the graph connectivity. Recall that GPCs also have a natural array representation: The code $\mathcal{C}_n(\boldsymbol{\eta})$ can alternatively be defined as the set of all code arrays of a given shape (see Fig. 1

for examples) such that each row and column is a codeword in some component code. Thus, one may alternatively think about $\boldsymbol{\eta}$ as specifying the array shape. We will see in the following that different choices for $\boldsymbol{\eta}$ recover well-known code classes.

A. Code Construction

Let $\gamma > 0$ be some fixed and arbitrary constant such that $d \triangleq \gamma n$ is an integer. To construct the Tanner graph that defines $\mathcal{C}_n(\boldsymbol{\eta})$, assume that there are L positions. Then, place d CNs at each position and connect each CN at position i to each CN at position j through a VN if and only if $\eta_{i,j} = 1$.

Example 1. A PC is obtained by choosing $L = 2$ and $\boldsymbol{\eta} = \begin{pmatrix} 0 & 1 \\ 1 & 0 \end{pmatrix}$. The two positions correspond to "row" and "column" codes. For $\gamma = 1$, the code array is of size $n \times n$. △

For a fixed n, the constant γ scales the number of CNs in the graph. This is inconsequential for the asymptotic analysis (where $n \to \infty$) and γ manifests itself in the DE equations merely as a scaling parameter. Its choice will become clear once we discuss the comparison of codes defined by different $\boldsymbol{\eta}$-matrices in Sec. III-A.

CNs at position i have degree $d \sum_{j \neq i} \eta_{i,j} + \eta_{i,i}(d-1)$, where the second term arises from the fact that we cannot connect a CN to itself if $\eta_{i,i} = 1$. The CN degree specifies the length of the component code associated with the CN. We assume that each CN corresponds to a t-erasure correcting component code. This assumption is relaxed in Sec. V.

B. Iterative Decoding

Suppose that a codeword of $\mathcal{C}_n(\boldsymbol{\eta})$ is transmitted over the BEC[1] with erasure probability $p = c/n$ for $c > 0$. The decoding is performed iteratively assuming ℓ iterations of bounded-distance decoding for the component codes associated with all CNs. Thus, in each iteration, if the weight of an erasure pattern for a CN is less than or equal to t, the pattern is corrected. If the weight exceeds t, we say that the component code declares a decoding failure in that iteration.

C. Density Evolution

We wish to characterize the decoding performance in the limit $n \to \infty$. To that end, assume that we compute

$$z^{(\ell)} = \Psi_{\geq t+1}(c\boldsymbol{B}\boldsymbol{x}^{(\ell-1)}), \text{ with } \boldsymbol{x}^{(\ell)} = \Psi_{\geq t}(c\boldsymbol{B}\boldsymbol{x}^{(\ell-1)}), \quad (1)$$

where $\boldsymbol{x}^{(0)} = \mathbf{1}_L$ and $\boldsymbol{B} \triangleq \gamma\boldsymbol{\eta}$. The main result is as follows.

Theorem 1. *Let the random variable W be the fraction of component codes that declare decoding failures in iteration ℓ. Then, W converges almost surely to $\frac{1}{L}\sum_{i=1}^{L} z_i^{(\ell)}$ as $n \to \infty$.*

Proof (Outline). The decoding can be represented by applying a peeling algorithm to the residual graph which is obtained from the Tanner graph by deleting known VNs and collapsing erased VNs into edges [3], [5], [14]. Our code construction is such that the residual graph corresponds to an inhomogeneous random graph [15]. The expected value of a suitably
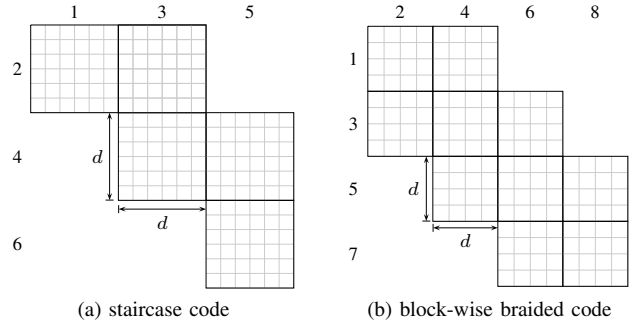
Fig. 1. Code arrays for $\mathcal{C}_{12}(\boldsymbol{\eta})$, where in (a) $\gamma = 1/2$ and in (b) $\gamma = 1/3$. Numbers indicate the position indices in the code construction.

defined function applied to such a graph converges to the expected value of the same function applied to a multi-type Poisson branching process [15]. One can show that the peeling algorithm constitutes a valid function and that $\frac{1}{L}\sum_{i=1}^{L} z_i^{(\ell)}$ corresponds to its expected value when applied to the branching process. Concentration is established by using the method of typical bounded differences [16]. For a complete proof we refer the reader to [17]. □

Th. 1 is analogous to the DE analysis for LDPC codes [12, Th. 2]. For notational convenience, we define $h(x) \triangleq \Psi_{\geq t}(cx)$, so that the recursion in (1) can be written as

$$\boldsymbol{x}^{(\ell)} = \boldsymbol{h}(\boldsymbol{B}\boldsymbol{x}^{(\ell-1)}). \quad (2)$$

Definition 1. The decoding threshold is defined to be

$$\bar{c} \triangleq \sup\{c \geq 0 \,|\, \boldsymbol{x}^{(\infty)} = \mathbf{0}_L\}. \quad (3)$$

III. SPATIALLY-COUPLED PRODUCT CODES

A. Deterministic Spatially-Coupled Product Codes

We are interested in cases where $\boldsymbol{\eta}$ (and hence $\boldsymbol{B}$) has a band-diagonal "convolutional-like" structure. The associated code can then be classified as a spatially-coupled PC.

Example 2. For $L \geq 2$, the matrix $\boldsymbol{\eta}$ describing a staircase code [4] has entries $\eta_{i,i+1} = \eta_{i+1,i} = 1$ for $i \in [L-1]$ and zeros elsewhere. The corresponding code array is shown in Fig. 1(a), where $L = 6$, $n = 12$, and $\gamma = 1/2$. △

Example 3. For even $L \geq 4$, let $\eta_{i,i+1} = \eta_{i+1,i} = 1$ for $i \in [L-1]$, $\eta_{2i-1,2i+2} = \eta_{2i+2,2i-1} = 1$ for $i \in [L/2-1]$, and zeros elsewhere. The resulting matrix $\boldsymbol{\eta}$ describes a particular instance of a block-wise braided code[2] [8]. The code array is shown in Fig. 1(b), where $L = 8$, $n = 12$, and $\gamma = 1/3$. △

The threshold $\bar{c}$ in Def. 1 is a function of $\boldsymbol{\eta}$ and the scaling parameter γ. A reasonable scaling to compare different spatially-coupled PCs is to choose γ such that $\lim_{L\to\infty} \frac{1}{L}\sum_{i=1}^{L}\sum_{j=1}^{L} B_{i,j} = 1$. For example, $\gamma = 1/2$ and $\gamma = 1/3$ for staircase and the above braided codes, respectively. This ensures that in both cases the component codes have length n, except at the array boundaries, see Fig. 1. The matrix $\boldsymbol{B}$ is then referred to as an averaging matrix.

---

[1]In practice, GPCs are used to correct errors and not erasures. However, the (rigorous) analysis over the BEC can be used to closely approximate the performance also over the binary symmetric channel, see, e.g., [3].

[2]We are somewhat liberal in our interpretation of the definition in [8] which is based on multiple block permutators. In [8], these permutators are linked to the dimension of the component code, which turns out to be unnecessarily narrow for our purposes.

B. Spatially-Coupled Product Code Ensembles

We wish to compare the obtained DE recursion in (2) to the DE recursion for the spatially-coupled PC ensemble defined in [13]. We review the necessary background in this section.

Let $\mathcal{B}$ be a t-erasure correcting component code of length n. The Tanner graph corresponding to one particular code in the spatially-coupled $(\mathcal{B}, m, L, w)$ ensemble, where L and w are referred to as the spatial length and coupling width, respectively, is constructed as follows (cf. [13, Def. 2]). Place m degree-n CNs corresponding to $\mathcal{B}$ at each position $i \in [L]$ and place $mn/2$ degree-2 VNs at each position $i \in [L']$, where $L' \triangleq L - w + 1$. The mn VN and CN sockets at each position are partitioned into w groups of mn/w sockets via a uniform random permutation. Let $\mathcal{S}_{i,j}^{(v)}$ and $\mathcal{S}_{i,j}^{(c)}$ be, respectively, the j-th group for the VNs and CNs at position i, where $j \in [w]$. The Tanner graph is constructed by connecting $\mathcal{S}_{i,j}^{(v)}$ to $\mathcal{S}_{i+j,w-j+1}^{(c)}$.

The ensemble-averaged performance for $m \to \infty$ is studied in [13]. Without going into the details, the obtained DE recursion in the high-rate regime (where, additionally, $n \to \infty$ and $p = c/n$) is given by [13, eq. (9)]

$$\tilde{\boldsymbol{x}}^{(\ell)} = c\boldsymbol{A}\boldsymbol{\Psi}_{\geq t}(\boldsymbol{A}^{\mathsf{T}}\tilde{\boldsymbol{x}}^{(\ell-1)}), \tag{4}$$

where $\tilde{\boldsymbol{x}}^{(0)} = c\boldsymbol{1}_{L'}$ and $\boldsymbol{A}$ is an $L' \times L$ matrix with entries

$$A_{i,j} = w^{-1}\mathbb{1}\left\{1 \leq j - i + 1 \leq w\right\}, \text{ for } i \in [L'], j \in [L]. \tag{5}$$

Remark 1. In [14], a modified spatially-coupled PC ensemble is considered. The obtained DE recursion is [14, eq. (4), $v = 2$]

$$\boldsymbol{y}^{(\ell)} = c\boldsymbol{A}^{\mathsf{T}}\boldsymbol{A}\boldsymbol{\Psi}_{\geq t}(\boldsymbol{y}^{(\ell-1)}), \tag{6}$$

which is identical to (4) choosing $\tilde{\boldsymbol{x}}^{(\ell)} = c\boldsymbol{A}\boldsymbol{\Psi}_{\geq t}(\boldsymbol{y}^{(\ell)})$.

Observe that (4) exhibits a double averaging due to the randomized edge connections for both VNs and CNs at each position. Using the substitution $\boldsymbol{x}^{(\ell)} = \boldsymbol{\Psi}_{\geq t}(\boldsymbol{A}\tilde{\boldsymbol{x}}^{(\ell-1)})$ with $\tilde{\boldsymbol{x}}^{(\ell)} = c\boldsymbol{A}\boldsymbol{\Psi}_{\geq t}(\boldsymbol{x}^{(\ell)})$, the recursion becomes

$$\boldsymbol{x}^{(\ell)} = \boldsymbol{\Psi}_{\geq t}(c\tilde{\boldsymbol{B}}\boldsymbol{x}^{(\ell-1)}) = \boldsymbol{h}(\tilde{\boldsymbol{B}}\boldsymbol{x}^{(\ell-1)}), \tag{7}$$

where $\boldsymbol{x}^{(0)} = \boldsymbol{1}_L$ and $\tilde{\boldsymbol{B}} \triangleq \boldsymbol{A}^{\mathsf{T}}\boldsymbol{A}$ is a symmetric $L \times L$ matrix. For $L = 6$, the $\tilde{\boldsymbol{B}}$-matrices for $w = 2$ and $w = 3$ are, respectively, given by

$$\frac{1}{4}\begin{pmatrix} 1 & 1 & 0 & 0 & 0 & 0 \\ 1 & 2 & 1 & 0 & 0 & 0 \\ 0 & 1 & 2 & 1 & 0 & 0 \\ 0 & 0 & 1 & 2 & 1 & 0 \\ 0 & 0 & 0 & 1 & 2 & 1 \\ 0 & 0 & 0 & 0 & 1 & 1 \end{pmatrix}, \quad \frac{1}{9}\begin{pmatrix} 1 & 1 & 1 & 0 & 0 & 0 \\ 1 & 2 & 2 & 1 & 0 & 0 \\ 1 & 2 & 3 & 2 & 1 & 0 \\ 0 & 1 & 2 & 3 & 2 & 1 \\ 0 & 0 & 1 & 2 & 2 & 1 \\ 0 & 0 & 0 & 1 & 1 & 1 \end{pmatrix}. \tag{8}$$

IV. COMPARISON OF DETERMINISTIC AND ENSEMBLE-BASED CODES

Comparing the equations, one finds that the ensemble DE recursion (7) has the same form as (2). The difference lies in the averaging due to the matrix $\tilde{\boldsymbol{B}}$.

Example 4. It can be shown that staircase codes are contained in the ensemble for $m = n/2$ and $w = 2$ using a proper choice of permutations. It is therefore tempting to conjecture

that for $w = 2$ the recursion (7) also applies to staircase codes. However, for staircase codes with $L = 6$, we have

$$\boldsymbol{B} = \gamma\boldsymbol{\eta} = \frac{1}{2}\begin{pmatrix} 0 & 1 & 0 & 0 & 0 & 0 \\ 1 & 0 & 1 & 0 & 0 & 0 \\ 0 & 1 & 0 & 1 & 0 & 0 \\ 0 & 0 & 1 & 0 & 1 & 0 \\ 0 & 0 & 0 & 1 & 0 & 1 \\ 0 & 0 & 0 & 0 & 1 & 0 \end{pmatrix}, \tag{9}$$

which is different from the matrix $\tilde{\boldsymbol{B}}$ for $w = 2$ in (8). $\triangle$

Example 5. For the braided codes in Ex. 3, one can simplify (2) by exploiting the inherent symmetry in the code construction, which implies $x_i^{(\ell)} = x_{i+1}^{(\ell)}$ for odd i and any ℓ. It is then sufficient to retain odd (or even) positions in (2). With this simplification, the effective averaging matrix[3] for $L = 12$ is

$$\boldsymbol{B}' = \frac{1}{3}\begin{pmatrix} 1 & 1 & 0 & 0 & 0 & 0 \\ 1 & 1 & 1 & 0 & 0 & 0 \\ 0 & 1 & 1 & 1 & 0 & 0 \\ 0 & 0 & 1 & 1 & 1 & 0 \\ 0 & 0 & 0 & 1 & 1 & 1 \\ 0 & 0 & 0 & 0 & 1 & 1 \end{pmatrix}, \tag{10}$$

where $\boldsymbol{B}'$ may be used to replace $\boldsymbol{B}$ in (2). Again, one finds that $\boldsymbol{B}'$ is different from the matrices $\tilde{\boldsymbol{B}}$ in (8). $\triangle$

A. Ensemble Performance via Deterministic Codes

Since $\boldsymbol{\eta}$ is binary, all entries in $\boldsymbol{B}$ are either zero or equal to γ. To construct spatially-coupled PCs that follow the same DE recursion as the ensemble, we need to "emulate" different multiplicities in the matrix $\boldsymbol{B}$. This is done as follows.

Definition 2. For given L and w, let $\gamma = 1/w^2$ and $\boldsymbol{P} = w^2\boldsymbol{A}^{\mathsf{T}}\boldsymbol{A}$, where $\boldsymbol{A}$ is defined by (5). We define $\boldsymbol{\eta}$ as follows. First, replace each entry $P_{i,j}$ in $\boldsymbol{P}$ by a symmetric $w \times w$ matrix with $P_{i,j}$ ones in each row and column. The resulting $wL \times wL$ matrix is denoted by $\boldsymbol{\eta}'$. Finally, $\boldsymbol{\eta}$ is given by

$$\eta_{2i,2j-1} = \eta'_{i,j}, \quad \eta_{2i-1,2j} = \eta'_{j,i}, \quad \text{for } i, j \in [wL]. \tag{11}$$

Example 6. Fig. 2 shows the (not necessarily unique) code array for $L = 6$ and $w = 3$, where $\boldsymbol{A}^{\mathsf{T}}\boldsymbol{A}$ is given in (8), which can be regarded as a type of braided code. $\triangle$

Using the structure of $\boldsymbol{\eta}$ in Def. 2, one can show that the DE recursion for $\mathcal{C}_n(\boldsymbol{\eta})$ in (2) is equivalent to (7). For example, the step in (11) is the opposite of the simplification in Ex. 5. The recursion defined by (7) constitutes an (unconditionally stable) scalar admissible system as defined in [10]. One may thus use the potential function approach in [10] to calculate decoding thresholds as follows (see also [5], [14]).

Definition 3. The single system potential function is defined as $V_s(x) \triangleq \frac{1}{2}x^2 - H(x)$, where $H(x) = \int_0^z h(z)\,\mathrm{d}z$. In order to highlight the dependence of the potential function on the channel quality parameter c, we write $V_s(x; c)$.

---

[3]The reader may wonder to what code the matrix (10) corresponds to, i.e., the code $\mathcal{C}_n(\boldsymbol{\eta})$ that results from using $\boldsymbol{\eta} = 3\boldsymbol{B}'$. One can show that $\mathcal{C}_n(\boldsymbol{\eta})$ can be interpreted as a symmetric subcode of the braided code, see [17], [18].
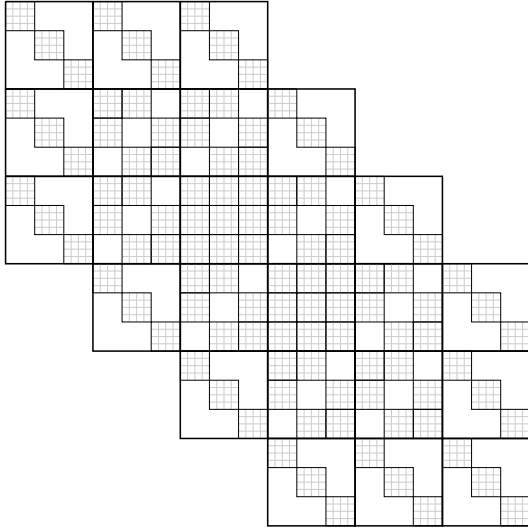
Fig. 2. Code array corresponding to $\mathcal{C}_{24}(\boldsymbol{\eta})$ in Def. 2 with $L = 6$, $w = 3$.

Definition 4. The potential threshold is defined as

$$\bar{c}_\mathrm{p} = \sup\{c \geq 0 \,|\, \min_{x \in [0;1]} V_s(x; c) \geq 0\}. \tag{12}$$

Using [10, Lem. 36], we have the following theorem.

Theorem 2. *Let $\boldsymbol{\eta}$ and γ be as in Def. 2. For any $c < \bar{c}_\mathrm{p}$, there exists $w_0 < \infty$ such that for all $w \geq w_0$ and all L, the DE recursion* (2) *for $\mathcal{C}_n(\boldsymbol{\eta})$ converges to the $\mathbf{0}$ vector.*

Remark 2. From Th. 2, the threshold of $\mathcal{C}_n(\boldsymbol{\eta})$ satisfies $\bar{c} \geq \bar{c}_\mathrm{p}$ for all L and w sufficiently large. One can further show that $\bar{c} \geq 2t - 2$ if, additionally, t is sufficiently large. The latter result was proved in [13, Lem. 8] for the spatially-coupled ensemble. It also applies to the deterministic braided codes in Def. 2, since the DE equations are equivalent.

B. Simpler Deterministic Codes

The curious structure of the code array in Fig. 2 is due to our attempt of "reverse-engineering" the DE equations of the ensemble by means of the deterministic code construction. This begs the question whether there exist other deterministic spatially-coupled PCs that exhibit a simpler structure but still achieve performance guarantees similar to those in Th. 2. The most natural candidate appears to be the extension of the block-wise braided code in Fig. 1(b) to larger coupling widths.

Definition 5. For given L and w, let $\gamma = (2w - 1)^{-1}$ and let the $L \times L$ matrix $\boldsymbol{\eta}'$ be defined by $\eta'_{i,j} = \mathbb{1}\{|i - j| < w\}$. Finally, let $\boldsymbol{\eta}$ be as in (11) for $i, j \in [L]$.

Example 7. For $w = 2$, $\boldsymbol{\eta}$ in Def. 5 recovers $\boldsymbol{\eta}$ in Ex. 3. $\triangle$

The resulting DE recursion for $\mathcal{C}_n(\boldsymbol{\eta})$ is neither equivalent to the ensemble DE recursion nor to the recursion studied in [10]. However, one can still show the following.

Theorem 3. *Let $\boldsymbol{\eta}$ and γ be as in Def. 5. For any $c < \bar{c}_\mathrm{p}$, there exists $w_0 < \infty$ such that for all $w \geq w_0$ and all L, the DE recursion* (2) *for $\mathcal{C}_n(\boldsymbol{\eta})$ converges to the $\mathbf{0}$ vector.*

Proof. See the Appendix. $\quad\square$

V. Potential Threshold Optimization

In this section, we consider the case where we assign different erasure-correcting capabilities to the component codes. To that end, let $\boldsymbol{\tau} = (\tau_1, \ldots, \tau_{t_\mathrm{max}})^\mathsf{T}$ be a probability vector (i.e., $\mathbf{1}^\mathsf{T}\boldsymbol{\tau} = 1$ and $\boldsymbol{\tau} \succeq 0$), where τ_t denotes the fraction of CNs at each position that can correct t erasures and t_max is the maximum erasure-correcting capability. We further define the average erasure-correcting capability as $\bar{t} \triangleq \sum_{t=1}^{t_\mathrm{max}} t\tau_t$. The assignment can be done either deterministically if $\tau_t d$ is an integer for all t, or independently at random according to $\boldsymbol{\tau}$. In both cases, the distribution $\boldsymbol{\tau}$ manifests itself in the DE equation (2) by changing the function h defined in Sec. II-C to $h(x) = \sum_{t=1}^{t_\mathrm{max}} \tau_t \Psi_{\geq t}(cx)$ (see [17] for details). This affects the potential function in Def. 3 and thus also the potential threshold in Def. 4. In particular, both quantities now depend on $\boldsymbol{\tau}$ and this change is reflected in our notation by writing $V_s(x; c, \boldsymbol{\tau})$ and $\bar{c}_\mathrm{p}(\boldsymbol{\tau})$, respectively.

Definition 6. A distribution is said to be regular if $\tau_{\bar{t}} = 1$ for $\bar{t} \in \mathbb{N}$ and semi-regular if $\tau_{\lfloor\bar{t}\rfloor} = 1 + \lfloor\bar{t}\rfloor - \bar{t}$ and $\tau_{\lfloor\bar{t}\rfloor+1} = \bar{t} - \lfloor\bar{t}\rfloor$ for $\bar{t} \notin \mathbb{N}$.

Theorem 4. *For any fixed mean erasure-correcting capability $\bar{t} \geq 2$, a (semi-)regular distribution maximizes the potential threshold $\bar{c}_\mathrm{p}(\boldsymbol{\tau})$.*

Proof. See the Appendix. $\quad\square$

Th. 4 is in contrast to conventional PCs which typically benefit from employing component codes with different strengths. However, Th. 4 does not necessarily imply that there can be no practical value in employing different component codes also for spatially-coupled PCs. In practice, quantities such as the coupling width, the component code length, and the number of decoding iterations are constrained to be finite. Depending on the severity of these constraints, the potential threshold may not be a good performance indicator.

VI. Conclusion

We studied the asymptotic performance of deterministic spatially-coupled PCs under iterative decoding. We showed that there exists a family of deterministic braided codes that performs asymptotically equivalent to a previously considered spatially-coupled PC ensemble. There also exists a related but structurally simpler braided code family that attains essentially the same asymptotic performance. Lastly, we showed that employing component code mixtures for spatially-coupled PCs is not beneficial from an asymptotic point of view.

Appendix

Proof of Theorem 3. The recursion of interest (after removing odd positions due to symmetry as explained in Ex. 5) is given by $\boldsymbol{x}^{(\ell)} = \boldsymbol{h}(\boldsymbol{B}'\boldsymbol{x}^{(\ell-1)})$, where $\boldsymbol{B}' = \gamma\boldsymbol{\eta}'$ and γ, $\boldsymbol{\eta}'$ are as in Def. 5. The authors in [10] study the recursion

$$\boldsymbol{y}^{(\ell)} = \boldsymbol{A}^\mathsf{T} \boldsymbol{f}(\boldsymbol{A}\boldsymbol{g}(\boldsymbol{y}^{(\ell-1)})) = \boldsymbol{A}^\mathsf{T} \boldsymbol{f}(\tilde{\boldsymbol{y}}^{(\ell)}) \tag{13}$$

for suitable functions f, g, where $\tilde{\boldsymbol{y}}^{(\ell)} = \boldsymbol{A}\boldsymbol{g}(\boldsymbol{y}^{(\ell-1)})$ is defined implicitly. Since h is strictly increasing and analytic,

we can let both $f = h$ and $g = h$. For this proof, $\boldsymbol{A}$ is assumed to be of size $L \times L + \tilde{w} - 1$ with $A_{i,j} = \tilde{w}^{-1}\mathbb{1}\{1 \leq j - i + 1 \leq \tilde{w}\}$ for $i \in [L]$, $j \in [L + \tilde{w} - 1]$, where $\tilde{w} \triangleq 2w - 1$. The potential function $U_s(x; c) = h(x)x - H(x) - H(h(x))$ associated with the scalar recursion $x^{(\ell)} = h(h(x^{(\ell-1)}))$ as defined in [10, eq. (4)] predicts the same potential threshold as the one in Def. 3. According to [10, Lem. 36], the claim in the theorem is thus true for the recursion (13). To show that it must also be true for the recursion of interest, we argue as follows. Assume that we swap the application of $\boldsymbol{h}$ and $\boldsymbol{B'}$ in the recursion of interest and then consider "two iterations at once" according to

$$\boldsymbol{z}^{(\ell)} = \boldsymbol{B'h}(\boldsymbol{B'h}(\boldsymbol{z}^{(\ell-1)})) = \boldsymbol{B'h}(\tilde{\boldsymbol{z}}^{(\ell)}). \tag{14}$$

We claim that (13) dominates (14), in the sense that $\boldsymbol{y}^{(\infty)} = \boldsymbol{0}$ implies $\boldsymbol{z}^{(\infty)} = \boldsymbol{0}$ (and thus $\boldsymbol{x}^{(\infty)} = \boldsymbol{0}$). To see this, observe that $\boldsymbol{y}^{(\ell)}$ has length $L + \tilde{w} - 1$, whereas $\tilde{\boldsymbol{y}}^{(\ell)}$, $\boldsymbol{z}^{(\ell)}$, and $\tilde{\boldsymbol{z}}^{(\ell)}$ have length L. We use $\boldsymbol{y}^{(\ell)} = ((\boldsymbol{y}_{\text{t}}^{(\ell)})^{\mathsf{T}}, (\boldsymbol{y}_{\text{c}}^{(\ell)})^{\mathsf{T}}, (\boldsymbol{y}_{\text{b}}^{(\ell)})^{\mathsf{T}})^{\mathsf{T}}$ to denote the $w - 1$ top, L center, and $w - 1$ bottom entries in $\boldsymbol{y}^{(\ell)}$. We want to show that $\boldsymbol{y}_{\text{c}}^{(\ell)} \succeq \boldsymbol{z}^{(\ell)}$ for all ℓ. Assume this is true for $\ell - 1$. This gives the second inequality in

$$\tilde{\boldsymbol{y}}^{(\ell)} = \boldsymbol{Ah}(\boldsymbol{y}^{(\ell-1)}) \succeq \boldsymbol{B'h}(\boldsymbol{y}_{\text{c}}^{(\ell-1)}) \succeq \boldsymbol{B'h}(\boldsymbol{z}^{(\ell-1)}) = \tilde{\boldsymbol{z}}^{(\ell)},$$

where the first inequality follows from $\boldsymbol{y}_{\text{t}}^{(\ell-1)}, \boldsymbol{y}_{\text{b}}^{(\ell-1)} \succeq \boldsymbol{0}$ (since $\boldsymbol{y}^{(\ell)} \succeq \boldsymbol{0}$ for all ℓ) and the (almost identical) structure of $\boldsymbol{A}$ and $\boldsymbol{B'}$. Observe that we have $\boldsymbol{y}_{\text{c}}^{(\ell)} = \boldsymbol{B'h}(\tilde{\boldsymbol{y}}^{(\ell)})$. Also $\boldsymbol{z}^{(\ell)} = \boldsymbol{B'h}(\tilde{\boldsymbol{z}}^{(\ell)})$ and, since we have just shown that $\tilde{\boldsymbol{y}}^{(\ell)} \succeq \tilde{\boldsymbol{z}}^{(\ell)}$, the claim follows by induction on ℓ. $\square$

Proof of Theorem 4. Using integration by parts, one may verify that the potential function in Def. 3 is given by

$$V_s(x; c, \boldsymbol{\tau}) = x^2/2 - x + (\bar{t} - \mathcal{L}_{\boldsymbol{\tau}}(cx))/c, \tag{15}$$

where we defined $\mathcal{L}_{\boldsymbol{\tau}}(x) \triangleq \sum_{t=1}^{t_{\max}} \tau_t \mathcal{L}(t, x)$, with $\mathcal{L}(t, x) \triangleq \sum_{k=0}^{t-1} \Psi_{=k}(x)(t - k)$ for $t \in \mathbb{N}$. For any fixed $x \geq 0$, we also define the affine extension of $\mathcal{L}(t, x)$ for $t \in [1, \infty)$ as

$$\mathcal{L}(t, x) = \mathcal{L}(\lfloor t \rfloor, x) + (\mathcal{L}(\lceil t \rceil, x) - \mathcal{L}(\lfloor t \rfloor, x))(t - \lfloor t \rfloor). \tag{16}$$

The proof relies on the fact that $\mathcal{L}(t, x)$ is convex in $t \in [1, \infty)$ for any $x \geq 0$. Indeed, since $\mathcal{L}(t, x)$ is the affine extension of a discrete function, it suffices to show that for $t \in \{2, 3, \dots\}$,

$$\mathcal{L}(t - 1, x) + \mathcal{L}(t + 1, x) = 2\mathcal{L}(t, x) + \Psi_{=t}(x) \tag{17}$$
$$\geq 2\mathcal{L}(t, x), \tag{18}$$

since $\Psi_{=t}(x) \geq 0$ with equality if and only if $x = 0$. As a consequence, for any distribution $\boldsymbol{\tau}$ with average erasure-correcting capability $\bar{t}$ and any $x \geq 0$, we have

$$\mathcal{L}_{\boldsymbol{\tau}}(x) \geq \mathcal{L}(\bar{t}, x) = \mathcal{L}_{\boldsymbol{\tau}_{\text{reg}}}(x), \tag{19}$$

where $\boldsymbol{\tau}_{\text{reg}}$ denotes the (semi-)regular distribution in Def. 6.

Now, let $\boldsymbol{t} \triangleq (1, 2, \dots, t_{\max})^{\mathsf{T}}$ and consider

$$\max_{\boldsymbol{\tau} \in \mathcal{T}} \bar{c}_{\text{p}}(\boldsymbol{\tau}) \text{ subject to } \boldsymbol{t}^{\mathsf{T}}\boldsymbol{\tau} = \bar{t}, \tag{20}$$

where $\mathcal{T} = \{\boldsymbol{\tau} \in \mathbb{R}^{t_{\max}} \mid \boldsymbol{1}^{\mathsf{T}}\boldsymbol{\tau} = 1, \boldsymbol{\tau} \succeq 0\}$. This can be equivalently written in epigraph form as

$$\max_{c \geq 0, \boldsymbol{\tau} \in \mathcal{T}} c \text{ subject to } c \leq \bar{c}_{\text{p}}(\boldsymbol{\tau}), \boldsymbol{t}^{\mathsf{T}}\boldsymbol{\tau} = \bar{t}. \tag{21}$$

According to (12), the first constraint in (21) is equivalent to $V_s(x; c, \boldsymbol{\tau}) \geq 0$ for $x \in [0; 1]$. Assume that (21) is maximized by some $(c^*, \boldsymbol{\tau}^*)$. Then, for all $x \in [0; 1]$, we have

$$0 \leq V_s(x; c^*, \boldsymbol{\tau}^*) \leq V_s(x; c^*, \boldsymbol{\tau}_{\text{reg}}), \tag{22}$$

where the last inequality follows from (15) and (19). Thus, the (semi-)regular distribution $\boldsymbol{\tau}_{\text{reg}}$ is feasible and attains (at least) the same threshold value c^*. $\square$

REFERENCES

[1] P. Elias, "Error-free coding," *IRE Trans. Inf. Theory*, vol. 4, no. 4, pp. 29–37, Apr. 1954.

[2] R. Tanner, "A recursive approach to low complexity codes," *IEEE Trans. Inf. Theory*, vol. 27, no. 5, pp. 533–547, Sep. 1981.

[3] J. Justesen, "Performance of product codes and related structures with iterated decoding," *IEEE Trans. Commun.*, vol. 59, no. 2, pp. 407–415, Feb. 2011.

[4] B. P. Smith, A. Farhood, A. Hunt, F. R. Kschischang, and J. Lodge, "Staircase codes: FEC for 100 Gb/s OTN," *J. Lightw. Technol.*, vol. 30, no. 1, pp. 110–117, Jan. 2012.

[5] Y.-Y. Jian, H. D. Pfister, K. R. Narayanan, R. Rao, and R. Mazahreh, "Iterative hard-decision decoding of braided BCH codes for high-speed optical communication," in *Proc. IEEE Glob. Communication Conf. (GLOBECOM)*, Atlanta, GA, 2014.

[6] L. M. Zhang and F. R. Kschischang, "Staircase codes with 6% to 33% overhead," *J. Lightw. Technol.*, vol. 32, no. 10, pp. 1999–2002, May 2014.

[7] C. Häger, A. Graell i Amat, H. D. Pfister, A. Alvarado, F. Brännström, and E. Agrell, "On parameter optimization for staircase codes," in *Proc. Optical Fiber Communication Conf. (OFC)*, Los Angeles, CA, 2015.

[8] A. J. Feltström, D. Truhachev, M. Lentmaier, and K. S. Zigangirov, "Braided block codes," *IEEE Trans. Inf. Theory*, vol. 55, no. 6, pp. 2640–2658, Jul. 2009.

[9] S. Kudekar, T. Richardson, and R. Urbanke, "Threshold saturation via spatial coupling: Why convolutional LDPC ensembles perform so well over the BEC," *IEEE Trans. Inf. Theory*, vol. 57, no. 2, pp. 803–834, Feb. 2011.

[10] A. Yedla, Y.-Y. Jian, P. S. Nguyen, and H. D. Pfister, "A simple proof of Maxwell saturation for coupled scalar recursions," *IEEE Trans. Inf. Theory*, vol. 60, no. 11, pp. 6943–6965, Nov. 2014.

[11] M. G. Luby, M. Mitzenmacher, and M. A. Shokrollahi, "Analysis of random processes via and-or tree evaluation," in *Proc. 9th Annual ACM-SIAM Symp. Discrete Algorithms*, San Franscisco, CA, 1998.

[12] T. J. Richardson and R. L. Urbanke, "The capacity of low-density parity-check codes under message-passing decoding," *IEEE Trans. Inf. Theory*, vol. 47, no. 2, pp. 599–618, Feb. 2001.

[13] Y.-Y. Jian, H. D. Pfister, and K. R. Narayanan, "Approaching capacity at high rates with iterative hard-decision decoding," in *Proc. IEEE Int. Symp. Information Theory (ISIT)*, Cambridge, MA, 2012.

[14] L. M. Zhang, D. Truhachev, and F. R. Kschischang, "Spatially-coupled split-component codes with bounded-distance component decoding," in *Proc. IEEE Int. Symp. Information Theory (ISIT)*, Hong Kong, 2015.

[15] B. Bollobás, S. Janson, and O. Riordan, "The phase transition in inhomogeneous random graphs," *Random Structures and Algorithms*, vol. 31, no. 1, pp. 3–122, Aug. 2007.

[16] L. Warnke, "On the method of typical bounded differences," *Combinatorics, Probability and Computing (to appear)*, 2015. [Online]. Available: http://arxiv.org/pdf/1212.5796.pdf

[17] C. Häger, H. D. Pfister, A. Graell i Amat, and F. Brännström, "Density evolution for deterministic generalized product codes on the binary erasure channel," *submitted to IEEE Trans. Inf. Theory*, 2015. [Online]. Available: http://arxiv.org/pdf/1512.00433.pdf

[18] H. D. Pfister, S. K. Emmadi, and K. Narayanan, "Symmetric product codes," in *Proc. Information Theory and Applications Workshop (ITA)*, San Diego, CA, 2015.